Michalowski, R. L. (1990). *Géotechnique* 40, No. 3, 389–403

Strain localization and periodic fluctuations in granular flow processes from hoppers

R. L. MICHALOWSKI*

Patterns of discharge processes of a granular material from plane containers are presented briefly. Rupture surfaces, interpreted here as shear bands, are a distinct feature of the flow patterns. Either a shock-like or a material character is attributed to the shear bands. A technique is shown for calculation of the energy dissipation rate within shear bands in softening materials. This technique is used in the limit analysis type of approach to the problem of extrusion of a strain-softening material through a pair of smooth flat dies, and to the discharge process of a granular material from a container. It is shown that the energy dissipation rate within a shear band in a non-steady (periodic) process may be lower than that in a steady-state flow. It is demonstrated that, if a criterion of minimum effort is used, periodic fluctuations in deformation patterns of softening materials can be predicted. The proposed analysis is size-sensitive; the scale effect is introduced through the assumption that the shear band thickness is a material property. It is essential for the analysis that deformation mechanisms are considered as processes, not as incipient flow mechanisms (which is the case in the classical kinematical approach of limit analysis).

KEYWORDS: granular materials; limit state analysis; plasticity; strain localization; periodicity.

L'article présent brièvement des types de processus de déchargement d'une matière granuleuse à partir d'un récipient plat. Des surfaces de rupture, interprétées comme des bandes de cisaillement, forment une caractéristique très marquée de ces types d'écoulement. On attribue aux bandes de cisaillement une nature analogue à un impact ou bien une nature materielle. Une technique est présentée pour calculer la vitesse de dissipation d'énergie à l'intérieur des bandes dans des matières qui se ramollissent. Cette technique est utilisée dans l'analyse limite appliquée à l'extrusion d'une matière qui se ramollit à travers une paire de matrices planes et lisses et aussi au processus de déchargement d'une matière granuleuse à partir d'un récipient. On montre que la vitesse de dissipation d'énergie a' l'intérieur d'une bande de cisaillement dans un processus non-stationnaire (périodique) peut être inférieure à celle dans un écoulement stationnaire. Il est démontré que si on emploie un critère d'effort minimal, des variations périodiques dans les types de déformation des matières qui se ramollissent peuvent être prédites. L'analyse proposée dépend des grandeurs, l'effet d'échelle étant introduit par l'hypothèse que l'épaisseur de la bande de cisaillement est une propriété du materiau. Pour cette analyse il est essentiel que les mécanismes de déformation soient considérés comme des processus et non comme des mécanismes naissants d'écoulement, comme dans le cas de la méthode cinématique traditionnelle d'analyse limite.

NOTATION

a, b, n, k_0	material constants
α	angle of inclination of a shear band
$\beta_1, \beta_2, \beta_3$	material constants
d	half-width of a bin
$\dot{D}$	rate of internal work dissipation
δ	shear band thickness
$\dot{\varepsilon}_{ij}$	strain-rate tensor
$\bar{\varepsilon}$	softening parameter (strain invariant)
$F = 0$	yield function
ϕ	angle of inclination of the velocity jump vector to the shear band
k	yield point
ψ	$\tan \psi = \sin \phi$
ρ	density of the material
ρ_{min}, ρ_{max}	physical limits of the density
s	$(\sigma_1 + \sigma_2)/2$
σ_{ij}	Cauchy stress tensor
t	real time
τ	$(\sigma_1 - \sigma_2)/2$
Θ	included semi-angle of a hopper
V^{in}	entry velocity of material with respect to a shear band
V^{out}	velocity of material leaving a shear band
$[V]$	total jump in the velocity vector across a shear band
V_0	velocity boundary condition

Discussion on this Paper closes 4 January 1991; for further details see p. ii.

* Johns Hopkins University, Baltimore.

x, y local co-ordinate system
$\dot{\omega}$ angular velocity of shear band rotation

INTRODUCTION

The flow of granular materials through plane-strain containers belongs to the class of problem where strain localization is a very distinct feature of the process. It may be beneficial, then, to study the process of the appearance and propagation of localized shear zones in containers, and to generalize some of the conclusions, as strain localization is a common phenomenon in granular materials, but it may not always be manifested as distinctly as it is in granular flow in containers.

It is not within the scope of this Paper to discuss criteria for bifurcation and strain localization. The rupture zones are considered here in relation to the kinematical approach of limit analysis, where they are a part of the assumed velocity fields. It will be shown that including the strain-softening characteristic of a material in the analysis may provide some valuable information, despite the fact that the upper and lower bound theorems do not hold for such materials.

Flow patterns during the discharge process of sand from a converging hopper and a parallel converging plane bunker will be presented in the next section. Two types of localized shear zone will be discussed in the section following that one, and an application of the results in a problem of extrusion of strain-softening material through a pair of smooth flat dies will be shown. Finally, a demonstration of the application of a density-softening model of granular material (in conjunction with shear bands formation) in predicting periodical fluctuations in the velocity field during the discharge process will be presented.

FLOW PATTERNS OF DISCHARGE PROCESSES FROM HOPPERS

It is not the objective of this section to present a comprehensive description of the velocity fields of plane-strain flow through containers. The purpose of presenting the velocity fields is only to study the experimentally observed behaviour of rupture surfaces (shear bands). A rather extensive list of publications concerned with the kinematics of granular materials in containers can be found in the review article by Tüzün, Houlsby, Nedderman & Savage (1982). The kinematical patterns shown in this section are based solely on the results presented earlier by the Author (Michalowski, 1984; 1987a).

Flow patterns presented here were obtained on plane-strain models whose height did not exceed 1·2 m, and width 0·4 m. The thickness of the models was 4 cm. Only qualitative conclusions were derived from the tests, and the influence of friction on the front and rear model walls was not analysed. Two types of container were tested: a straight-wall converging hopper and a parallel–converging bunker (hopper–bin container). In both cases sand was used with a particle size range of 0·25–1·75 mm.

The characteristic feature of the velocity fields was the appearance of discontinuities in the form of narrow zones with large velocity gradients. These discontinuities, located by means of stereophotographic technique, are marked by solid lines in Fig. 1 and Fig. 2. Dashed lines show discontinuities that were less distinct in the stereophotographic image. On initialization of flow in both the converging hopper and parallel-converging bunker, a symmetrical pair of narrow shear zones is created in the neighbourhood of the outlet. These zones cross each other somewhere around the axis of symmetry of the container and then reach the walls. Subsequently, a new pair of discontinuities starts from points where the previous pair reached the walls.

This process repeats itself until the discontinuities reach the free boundary in the converging hopper or the transition zone in the parallel-converging bunker. While new discontinuities are being created in the upper part of the container,

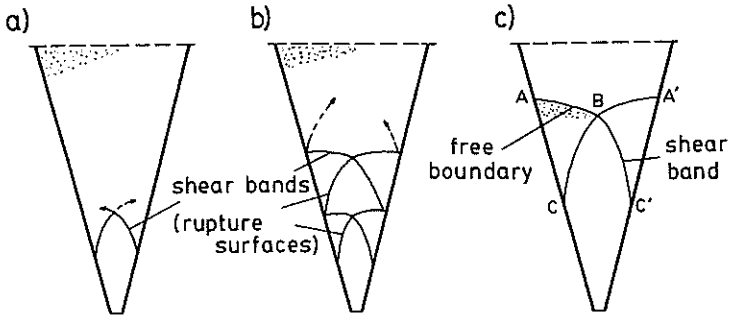

Fig. 1. Rupture surfaces during discharge flow from plane-strain wedge-shaped hopper model: (a), (b) initial phase; (c) advanced flow

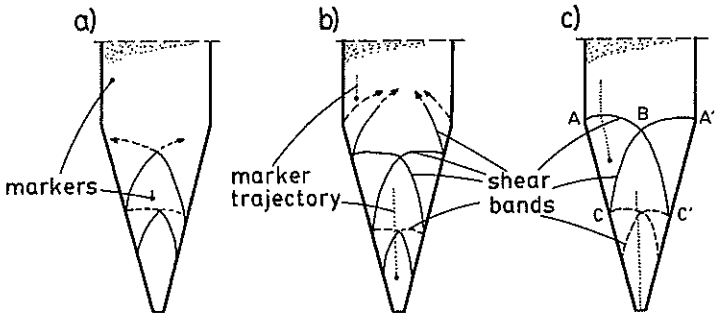

Fig. 2. Rupture surfaces during discharge flow from plane-strain parallel–converging bunker model: (a), (b) initial; (c) advanced flow

the discontinuities below remain active, but they do not remain stationary; they move down. However, it was difficult to determine whether these discontinuities had the character of material zones or moved with a velocity different from that of the material. This difficulty comes from the fact that only the displacement field could be measured, and its interpretation as a velocity field is only approximate, especially when the velocity field is not steady and the velocity gradients are high (inside the shear zones).

The advanced phase of flow is shown in Fig. 1(c) and Fig. 2(c), respectively. The shape of the free boundary and the shear zones in the converging hopper stay (approximately) geometrically similar until the top pair of discontinuities reaches the neighbourhood of the outlet. Stereophotographic observations of the velocity field throughout the advanced phase of flow in the parallel–converging bunker seem to suggest that the geometry of the velocity field remains stationary. It will be shown later, however, that this field undergoes periodic fluctuations.

The type of pattern shown in Fig. 1 and Fig. 2 is usually referred to in the literature as the mass flow. For some combinations of geometrical parameters of the container and properties of the granular media, the flow pattern may be quite different, and it will be referred to here as the funnel flow. A characteristic feature of funnel flow is that, on initialization of the discharge process, the material starts to flow only in a narrow core (Fig. 3). The upper boundary of this core propagates upwards with a relatively high speed (the speed of upward propagation of the core is about one order higher than the velocity of the material inside the core). The speed of expansion of the core in the horizontal direction (towards the walls) is lower and is of the same order of magnitude as the velocities of the material particles. The funnel type of flow may appear in both converging hoppers and hopper–bin containers. Piping and arching in containers are not considered here, as they are not of interest from the point of view of shear band formation.

Figures 4–6 show X-radiographs of the models. Fig. 4 represents the initial stage of the mass-flow process from a converging hopper, and Fig. 5 shows the density distribution during funnel flow. It is clearly demonstrated on the X-radiographs

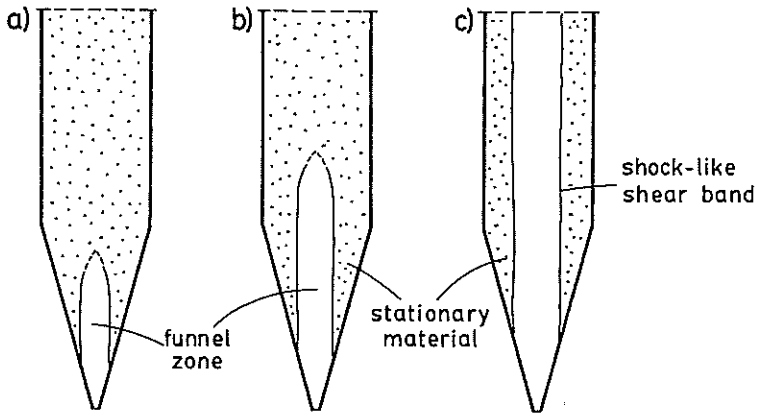

Fig. 3. Funnel flow discharge pattern in converging wedge-shaped hopper

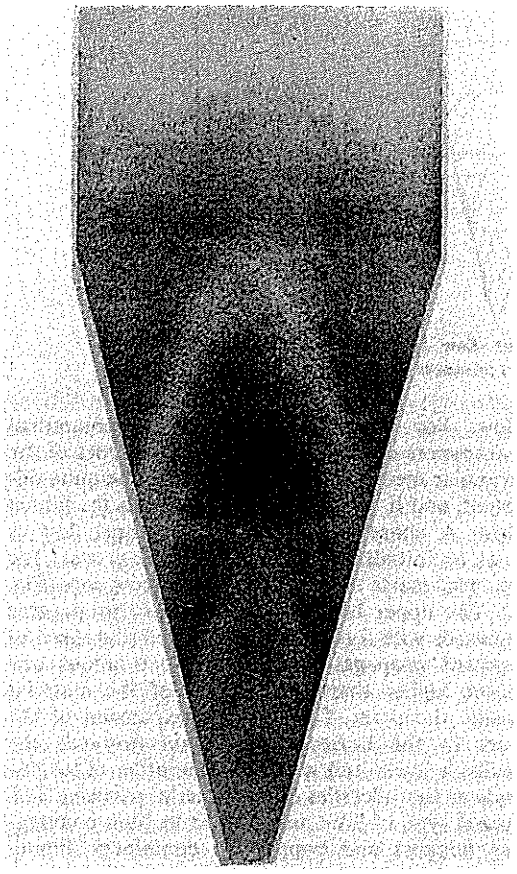

Fig. 4. X-radiograph of initial stage of flow from converging hopper

that the material undergoes dilation while being sheared in the narrow zones coinciding with the so-called rupture surfaces. The X-radiograph in Fig. 6 seems to be the most interesting of all. It was taken during the advanced phase of discharge from a parallel–converging bunker model. The image of the densities exhibits a periodic structure (alternate layers of loose and dense material) in the regions corresponding to the ABC and A′BC′ areas in Fig. 2(c). However, only the top pair of the narrow dilated zones are active discontinuities (shear layers) in the velocity field. The X-radiograph in Fig. 6 does not represent the image of the incipient flow but a well-advanced deformation process. The appearance of the periodically spaced layers of loose material is related to fluctuations in the velocity field during the advanced flow phase. It will be shown later in this Paper that a simple limit plasticity approach may be helpful in predicting such perturbations in the deformation patterns.

A more elaborate description of flow patterns shown here, and documented experimental results, can be found elsewhere (Michalowski 1984; 1987a).

SHOCK-LIKE DISCONTINUITIES AND MATERIAL SHEAR BANDS

Two types of discontinuity layer can be distinguished in the patterns presented. The first type can be clearly observed in the funnel flow mechanism (Figs 3 and 5). The vertical boundary that separates the material in the flowing core from the stationary material moves with a velocity different from the velocity of the particles on either side. This discontinuity has a finite thickness and has the character of a shock in the deformation field; it will be referred to here as a shock-like shear band. A shock-like interpretation of discontinuities in granular material velocity fields was suggested earlier by Drescher and Michalowski (1984). The shear bands shown in Fig. 1(c) also have a shock-like character. It is clear that regions ABC and A′BC′ in Fig. 1(c) have to reduce as the process advances, so the material particles jump across bands BC and BC′.

A characteristic feature of shock-type shear bands is that the velocities of the material (measured with respect to the velocity of the band) are different from zero on both sides of the band. It was impossible to detect from the experiments whether or not these bands have a constant thickness. Displacement fields from the stereophotographic measurements cannot be strictly identified with the velocity fields, and the thickness of dilated (loosened) layers on the X-radiographs cannot be identified with the thickness of the shear bands. Assuming that an observer moves with the shock bands (bounding the funnel zone, Fig. 3 and Fig. 5) the velocity field with respect to this observer seems to be stationary in the neighborhood of the shock. Therefore it is assumed here that the shock-like bands have a constant thickness. This thickness will be considered here as material property.

A shock-like shear band is shown in Fig. 7(a). The material particles enter the band with velocities $\boldsymbol{V}^{in}$, undergo acceleration within the band, and leave the shear band with velocity

$$\boldsymbol{V}^{out} = \boldsymbol{V}^{in} + [\boldsymbol{V}] \tag{1}$$

$[\boldsymbol{V}]$ being the total jump of the velocity across the shear band.

The second type of discontinuity layer considered here is a material shear band (Fig. 8). Unlike in the case of shock-type bands, the boundaries of the material shear band are stationary with respect to the material outside the band; there is no material entering or leaving the shear band. The shear band thickness in a defor-

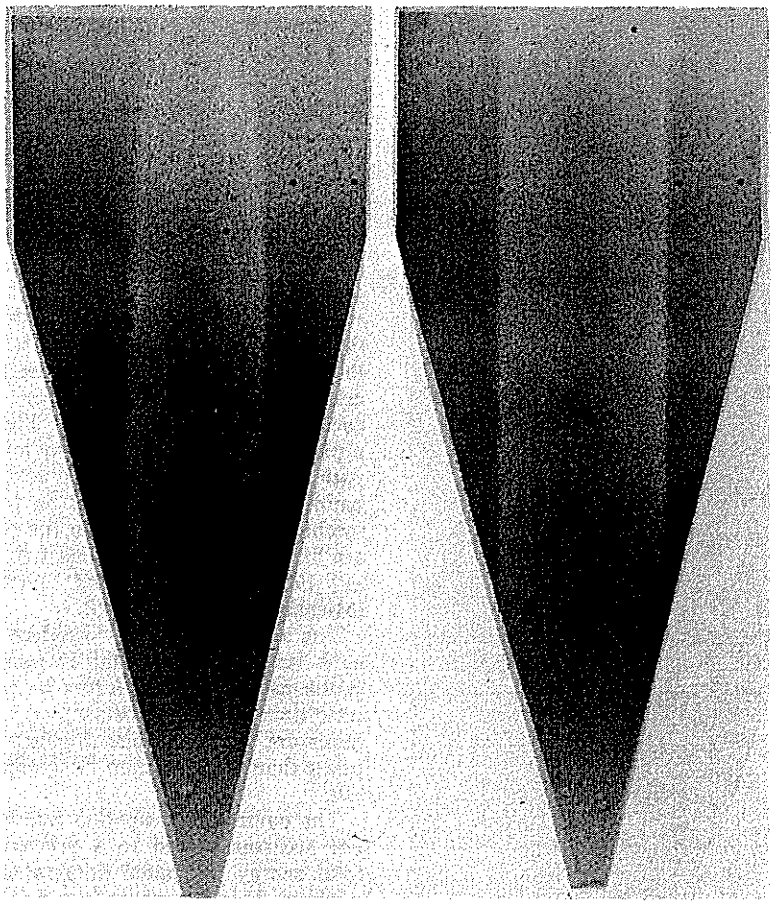

Fig. 5. X-radiographs of a funnel-flow mechanism in converging hopper model

mation process increases in dilating materials, and the density of the material within the band decreases.

Material shear bands are often observed in biaxial and triaxial tests of soils in the post-bifurcation regime (e.g. Vardoulakis, 1980). It will be shown here that if a material character is attributed to shear bands AB and A'B (Fig. 2(c)), periodic fluctuations in the velocity field can be predicted and the dense–loose layered structure of the density field (Fig. 6) can be explained.

HYPOTHESIS FOR PREDICTING PERTURBATIONS IN VELOCITY FIELDS

It has been known for quite some time now that localization of strain within a plastically deforming material may take place even under conditions of a homogeneous stress state. Criteria for occurrence of strain localization were discussed by Rudnicki & Rice (1974), Hill & Hutchinson (1975), Vardoulakis (1980), Vermeer (1982), and others. Here, based on experimental data, it is assumed that localization of strain takes place during discharge from hoppers. It will be demonstrated, however, that minimizing the rate of energy dissipation within shear bands may provide valuable information regarding periodic fluctuations of the velocity field.

The criterion of minimum energy dissipation is often used in plastic forming of metals. If the body forces are neglected, for any admissible deformation mechanism the external effort (work) is equilibrated only by the internally dissipated energy. Further, if the material is perfectly plastic and obeys a convex yield condition and the flow rule associated with this condition, such approach yields an upper bound to the true limit load (or external effort). Thus, by minimizing the internal energy dissipation, an approximate solution to the limit load problem can be found. A similar approach was applied earlier to strain-hardening metals. The theorems of limit analysis do not hold for hardening–softening materials;

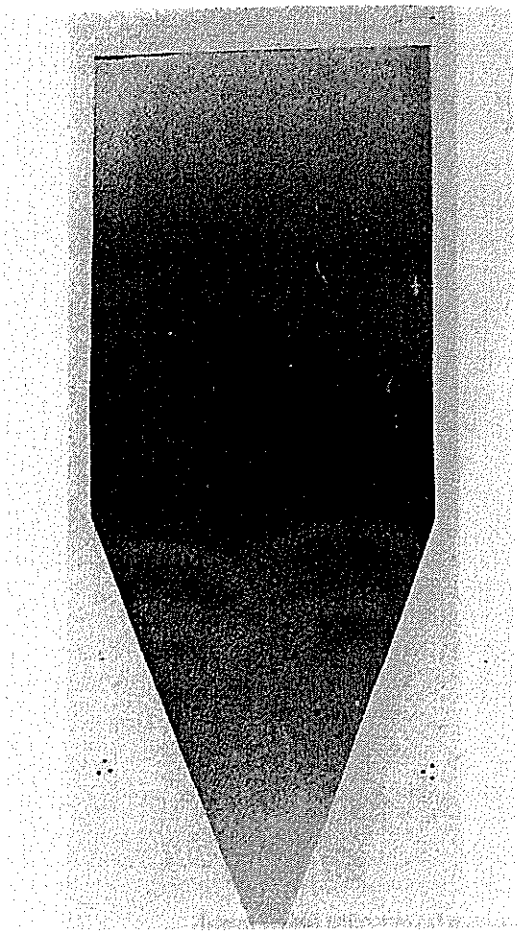

Fig. 6. X-radiograph of advanced discharge process from parallel–converging bunker model

however, the results obtained (Michalowski, 1986) seem to suggest that this method may be a valuable engineering tool for such materials. This method was also used by Drescher and Kang (1987) for evaluating penetration forces of hardening soils. Here it is applied to predict perturbations in the velocity field.

The reasoning is as follows: a kinematically admissible steady-state deformation field is assumed, the rate of internal energy dissipation is calculated, and the (stationary) geometry of the mechanism is found for which the rate of dissipation reaches its minimum. Next, a perturbation of the mechanism is assumed in which the discontinuities (shear bands) in the mechanism are allowed to propagate in space. This causes the strain rates within the shear bands, and thus also the energy dissipation rates, to be different from those in the steady-state mechanism. It is assumed that the mechanism generating the least energy dissipation rate is most likely to appear in a physical process. Thus, if the level of the dissipation rate in the mechanism undergoing perturbations is lower than that in the steady-state mechanism, perturbations in the physical process are likely to occur. This idea was first presented in 1987, and discussed further in 1989 (Michalowski, 1987b; 1989).

The above should be considered a hypothesis, as it lacks a mathematically rigorous proof. In problems where body forces or stress boundary conditions are important, a hypothesis of minimum applied (external) effort is more appropriate than the minimum dissipation rate hypothesis.

The minimum dissipation rate hypothesis does not necessarily lead to a process in which the total energy dissipated (integrated over time) is minimal. This is because in a non-steady process the rate of energy dissipation may increase while the process progresses. However, switching to another process (with a lower dissipation rate) may be kinematically inadmissible once a particular deformation pattern has already developed.

EXTRUSION OF STRAIN-SOFTENING MATERIAL THROUGH SMOOTH FLAT DIES

Before the analysis of sand flowing through a plane hopper–bin container is presented, a related

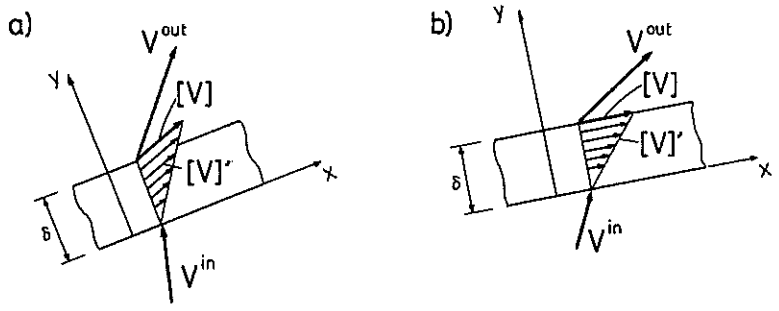

Fig. 7. Shock-like shear bands with constant strain-rate across thickness δ: (a) in dilating material; (b) incompressible material

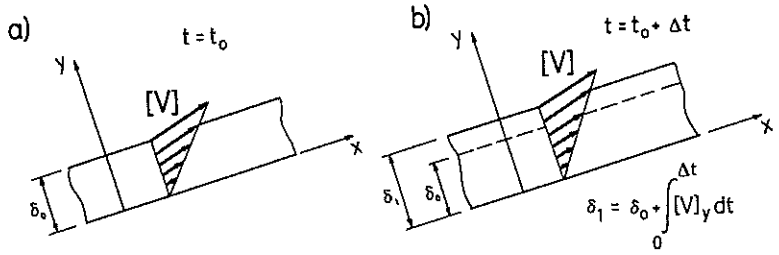

Fig. 8. Material shear band (dilating material): (a) at time $t = t_0$; (b) at $t = t_0 + \Delta t$

problem for an incompressible strain-softening material is considered. Fig. 9(a) shows a kinematically admissible velocity field of an extrusion through a symmetrical pair of smooth dies (plane strain). The following is not a rigorous solution to the extrusion problem, but only a demonstration of the applicability of the proposed analysis in predicting periodic fluctuations in the velocity fields in strain-softening materials. Therefore, to reduce the number of computations, only the dissipation rates generated by bands AB and A'B (Fig. 9(a)) will be calculated.

Consider a shock-like shear band of thickness δ, with linearly distributed velocity jump $[V]$ (Fig. 7(b))

$$[V]' = [V](y/\delta) \tag{2}$$

where $[V]$ is the length of vector $[V]$ and y is the co-ordinate of the local system (see Fig. 7(b)). The material is assumed to obey the Tresca yield condition, but yield point k is the decreasing function of strain

$$k = k_0 - b(1 - e^{-a\bar{\varepsilon}}) \tag{3}$$

where k_0, b and a are the material parameters. The material is assumed to be incompressible (associated flow rule), thus, vector $[V]$ is parallel to the shear band; $\bar{\varepsilon}$ is defined here as

$$\bar{\varepsilon} = \sqrt{(\tfrac{2}{3}\varepsilon_{ij}'\varepsilon_{ij}')}, \quad \varepsilon_{ij}' = \varepsilon_{ij} - \tfrac{1}{3}\varepsilon_{kk}\,\delta_{ij} \tag{4}$$

where ε_{ij} is the strain tensor (for an incompressible material $\varepsilon_{ij} = \varepsilon_{ij}'$). For the particular case considered here (steady-state) the distribution of $\bar{\varepsilon}$ across the shear band is

$$\bar{\varepsilon} = \frac{2}{\sqrt{3}}\,\varepsilon_{xy} = \frac{1}{\sqrt{3}}\,\frac{[V]}{V_y^{in}}\,\frac{y}{\delta} \tag{5}$$

V_y^{in} is the component of vector V^{in} (Fig. 7) and δ is the thickness of the shear band. Equation (5) was arrived at by integrating the strain rate, $\dot{\varepsilon}_{xy} = [V]/2\delta$, over time t spent by a material element inside the shear band, $t = y/V_y^{in}$ ($\dot{\varepsilon}_{xy}$ is constant within the shear band due to assumed linear distribution of $[V]$, and is constant in time for the steady state process). The rate of work dissipation per unit area of the shear band (in the $x0z$ plane) can be expressed as

$$\dot{D} = \int_0^{\delta} \sigma_{ij}\,\dot{\varepsilon}_{ij}\,dy \tag{6}$$

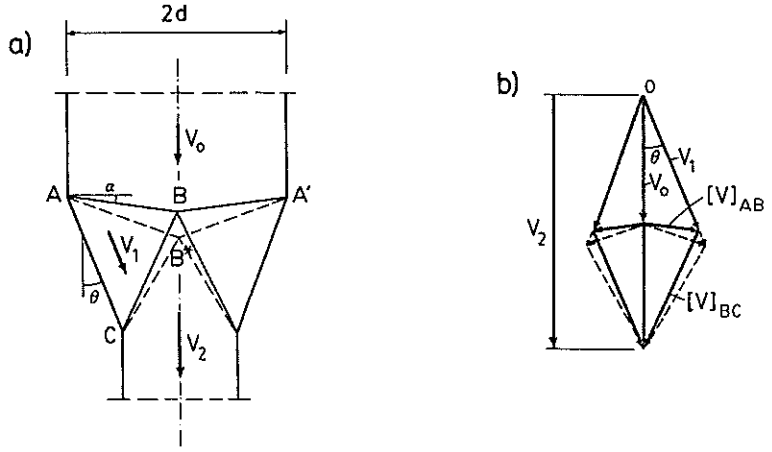

Fig. 9. (a) Kinematically admissible velocity field for plane-strain extrusion problem through pair of symmetrical dies; (b) hodograph (V_0 is velocity boundary condition)

For an incompressible material and constant shear strain-rate across thickness δ, Equation (6) can be written as

$$\dot{D} = [V]\frac{1}{\delta}\int_0^{\delta} k(\bar{\varepsilon})\, dy \tag{6a}$$

and, after utilizing Equation (3)

$$\dot{D} = (k_0 - b)[V] + \sqrt{3}\,\frac{b}{a}\,V_y^{in} \times \left[1 - \exp\left(-\frac{a}{\sqrt{3}}\,\frac{[V]}{V_y^{in}}\right)\right] \tag{7}$$

The total dissipation rate within stationary shear band AB (Fig. 9(a)) now can be found by integrating Equation (7) along AB (multiplying by distance AB). Angle α corresponding to the minimum of the total dissipation rate (in the steady-state process) can be obtained using a numerical procedure minimizing the dissipation rate function (minimum effort hypothesis).

The total dissipation rate along band AB in the steady-state process is represented by the horizontal section of the continuous diagram in Fig. 10(a). The ordinate denotes the dimensionless dissipation rate, and the abscissa shows the advancement of the process (dimensionless time). V_0 is the velocity boundary condition (Fig. 9(a)). The dissipation in the steady-state process is constant. The first section of the continuous diagram corresponds to initial phase of the process where the virgin material (not yet softened) fills the shear band.

Consider now a small perturbation of the mechanism, shown in Fig. 9(a), where the end point of shear band AB moves from position B to B* in time increment Δt. This causes rotation of

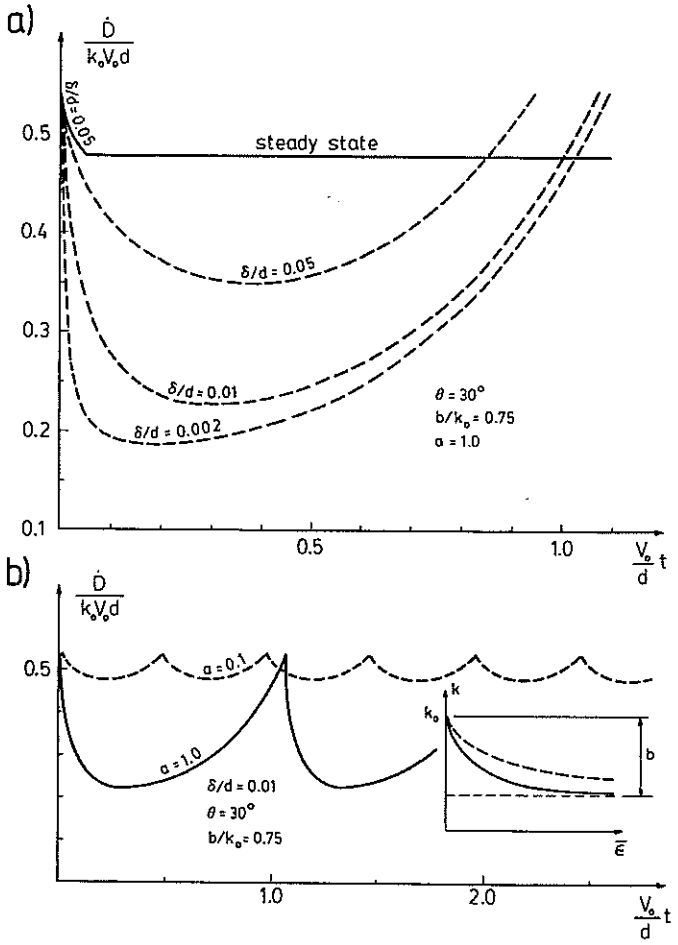

Fig. 10. (a) Work dissipation rate (dimensionless) integrated along shear band AB (Fig. 9(a)) as function of process advancement (internal time); (b) cyclic fluctuations in work dissipation rate for two strain softening materials with different rates of softening

shear band AB around point A. Such mechanism is kinematically admissible. Velocity jump vector $[V]$ across AB can be calculated for any position of AB (hodograph, Fig. 9(b)). Velocity V_y^{in} will vary now due to variation in the mechanism's geometry (angle α) and due to the fact that it is measured with respect to the (moving) shear band

$$V_y^{in} = V_0 \cos \alpha - \dot{\omega} x \tag{8}$$

This causes the strain rates to vary along the shear band, and, as long as the rotational velocity $\dot{\omega}$ of shear band AB is clockwise, the strain rates will be higher than those in a stationary shear band. Therefore, for a strain-softening material, it is reasonable to expect a decreasing dissipation rate with its gradient at $t = 0$ steeper than that for a stationary band. On the other hand, due to geometrical changes, the dissipation rate will gradually increase (the position of the shear band at $t = 0$ corresponds to minimum dissipation in the steady state process). Therefore, one should expect the dissipation rate function to have a minimum with respect to time.

Dissipation rates for a non-steady process as functions of dimensionless (internal) time are represented in Fig. 10(a) by the dashed lines. These dissipation rates cannot be obtained by simply integrating (7) over shear band length AB with V_y^{in} described by Equation (8). The process is now non-steady and the profile of material strains across the shear band thickness changes as the process advances. The calculations were performed numerically.

The shear band was divided into ten elements and the process was divided into small time increments ($\Delta V_0 t/d = 5 \times 10^{-4}$). Strain increments were then calculated across each element, and integrated at every time step, so the current yield point distribution across the elements could be calculated according to Equation (3). Note that V_y^{in} changes according to Equation (8), where angle α (see also Fig. 9(a)) is updated at every time step ($d\alpha = \dot{\omega}\, dt$). Next, the work dissipation rate was numerically integrated within each element (Equation (6)) and summed over all the elements.

As opposed to the steady-state solution, the dissipation rate is not constant in time and it depends on thickness δ of the shear band. This is a clear scale effect introduced into the analysis through the assumption that the thickness of the shear band is a material property (independent of the size of the boundary value problem). Thickness δ can be regarded as an internal length parameter.

The scale effect was not present in the steady-state solution. In steady-state flow across a (shock-like) shear band of any thickness δ, the distribution of strains (and, thus, the yield point) is identical (for a given $[V]$) if normalized with respect to δ. The work dissipation rate, as the integral over the shear band thickness, is then independent of a specific δ, since the strain-rate components are inverse functions of δ. This is not the case when a non-steady process takes place. In the latter, the distribution of strains across thickness δ is piece-wise linear and its gradient in the part (say δ_1) occupied by the material which has entered the shear band (with velocity V^{in}) is different from that in the part (δ_2) occupied by the material which has been associated with the shear band from the instant the shear band was formed. The magnitudes of the material strain and the ratio δ_1/δ_2 depend on the time lapsed and total thickness δ, thus the work dissipation rate is also a function of time and total thickness of the shear band, unlike in steady-state flow.

According to the hypothesis described in the previous section, one should expect the physical experiment to follow the non-steady dissipation curve since it produces lower energy dissipation rates at the beginning of the process. After the energy dissipation rate reaches its minimum, it increases to the level of the initial value. At this point a new shear band will be formed, as it requires dissipation rates lower than those required to continue the process. The new shear band will be formed at the same spatial location where the first one started, and the first one will stop acting as a shear band. Therefore the process is likely to exhibit periodical fluctuations in the velocity field.

Periodic variations of the dissipation rate within moving shear band AB (Fig. 9(a)) are shown in Fig. 10(b). The length of the cycle depends on both the thickness of the shear band and on the rate of material softening.

Velocity $\dot{\omega}$ of the shear band rotation was not given *a priori*. This velocity was determined from the requirement of the minimum dissipation rate and was such that it produced a translation of the shear band in the symmetry axis equal to the displacement of the material (highest admissible $\dot{\omega}$). Therefore the shear bands considered here were essentially shock-type in character.

If a solution to the entire problem was sought (dissipation within the whole mechanism), then the computations would be far more elaborate, as the material below the first shear band is non-homogeneous. The basic properties of the solution (periodic fluctuations) would stay the same, however.

PERIODIC PERTURBATIONS IN FLOW THROUGH BUNKER

The density distribution of sand during the advanced discharge process from a plane

parallel–converging bunker is shown in Fig. 6. It is seen clearly that the layers of dense and loose material appear alternately in regions ABC and A'BC' (cf. Fig. 2(c)); these layers seem to be parallel to each other. Only the top pair of loosened layers coincides with the shear bands (AB and A'B, Fig. 2(c)). An oscillatory mechanism of forming the shear bands can explain the development of the alternate loose and dense layers (Michalowski, 1987a). The dense material that is fed from the bin part into the transition zone undergoes dilation within the top pair of shear bands. Such dilation effect is expected to take place in a dense granular (pressure-sensitive) material. These shear bands do not remain at their spatial location during the flow process. They move downwards until a new pair of shear bands is created above them, leaving a strip of undilated material in between. When a new pair of shear bands is created, the first pair stops acting as such. This process is continuously repeated, leaving the layers of loose and dense material in regions ABC and A'BC' (cf. Fig. 2(c) and Fig. 6). Below these regions the material is homogenized owing to further deformation along bands BC and BC'.

It will be demonstrated in this section that, if the hypothesis of minimum material effort (or minimum dissipation rate) is adopted, the cyclic fluctuations in the velocity field can be predicted through the use of a simple limit analysis approach.

The material is described here by a density-hardening–softening model with yield surfaces $F(\sigma_{ij}, \rho) = 0$ shown in Fig. 11(a). The material is assumed to be continuous, so physical relations can be described in terms of stresses and strains. $\beta_1, \beta_2, \beta_3$ and k are material parameters describing the yield condition. Only parameter k is dependent on density ρ, (Fig. 11(b))

$$k = a(\rho/\rho_{max})^n - b \tag{9}$$

a, n, b and ρ_{max} are the material constants, ρ_{max} being the maximum possible bulk density for the given material (corresponding to minimum porosity). It is further assumed that there exists a minimum bulk density ρ_{min}. The density of the material during plastic flow cannot drop below ρ_{min}, and $k = 0$ at $\rho = \rho_{min}$. Thus b in function (9) is not an independent parameter and can be expressed as

$$b = a(\rho_{min}/\rho_{max})^n \tag{10}$$

The material is assumed to obey the associated flow rule

$$d\varepsilon_{ij} = d\lambda \frac{\partial F}{\partial \sigma_{ij}}, \quad d\lambda \geqslant 0 \tag{11}$$

where $d\varepsilon_{ij}$ is the strain increment tensor, σ_{ij} is the stress tensor, $F = F(\sigma_{ij}, \rho) = 0$ is the yield condition for the material and $d\lambda$ is a non-negative increment of a scalar function λ. Variation of density is dependent on volume strain increment $d\varepsilon_{ii}$

$$d\rho = -\rho\, d\varepsilon_{ii} \tag{12}$$

Function λ in flow rule (11) can be determined using condition $dF(\sigma_{ij}, \rho) = 0$ for active plastic processes, and relation (12). This is not done here, because, in the kinematical approach used, the velocity field is assumed *a priori*, and flow rule (11) is used only to assure kinematical admissibility of deformation within the shear band.

A kinematical mechanism for discharge from a plane bunker consisting of a parallel bin and

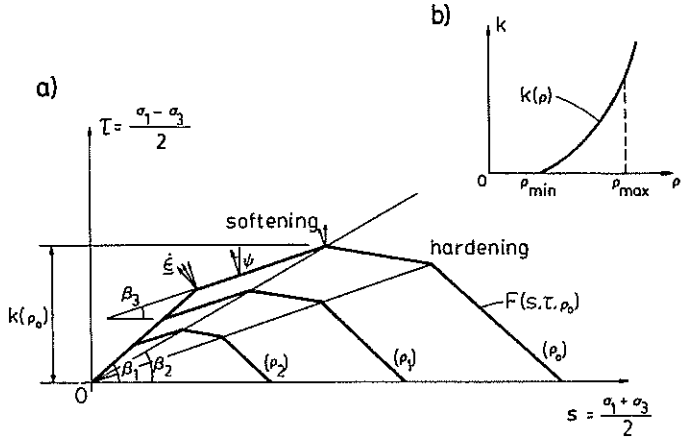

Fig. 11. (a) Yield surfaces as functions of density; (b) parameter k as function of density ρ

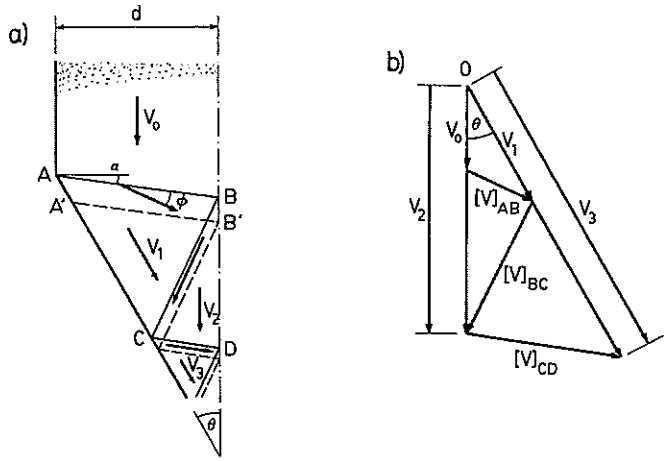

Fig. 12. (a) Kinematical mechanism for discharge problem; (b) hodograph. (It is assumed that material dilates only along shear band AB)

wedge-shaped hopper is shown in Fig. 12(a). First, steady-state flow is considered. The material moves down in the bin with velocity V_0 (the boundary condition), it jumps across the top shock-like shear band (AB), moves parallel to the hopper wall, then crosses the next shock-like shear band (BC), moves vertically downwards within area BCD, crosses shear band CD and so on. This mechanism, despite its simplicity, is a close approximation of mechanisms observed in experiments. As in the case of the extrusion problem presented in the previous section, only the dissipation rate within shear band AB is analysed.

Total velocity jump $[V]$ across shear layer AB can be determined from the hodograph, Fig. 12(b). Vector $[V]$ is inclined at angle ϕ to band AB. This inclination is related to ψ with the relation $\sin\phi = \tan\psi$ (ψ shown in Fig. 11(a)). Both angle ψ and angle α (inclination of shear band AB) are not given *a priori*, and will be found from the requirement of the minimum dissipation rate.

Consider now a shock-like band (Fig. 7(a)) with a linear distribution of velocities in the y-direction

$$\left.\begin{aligned} V_x &= V_x^{in} + \frac{[V]\cos\phi}{\delta}\, y \\ V_y &= V_y^{in} + \frac{[V]\sin\phi}{\delta}\, y \end{aligned}\right\} \tag{13}$$

In steady-state flow of the material across the band the volume strain is

$$\varepsilon_s = \varepsilon_{ii} = \int_0^t \dot{\varepsilon}_{ii}\,dt = \int_0^y \dot{\varepsilon}_{ii}\frac{dy}{V_y} = \ln\left|1 + \sin\phi\,\frac{[V]}{V_y^{in}}\,\frac{y}{\delta}\right| \tag{14}$$

where t is the time in which a material element moves inside the band from position $y = 0$ to y ($y \leqslant \delta$). Using relation (12) the distribution of density across the shock-like band can be found, ρ_0 being the initial (inflow) density of the material

$$\rho = \rho_0\left(1 + \sin\phi\,\frac{[V]}{V_y^{in}}\,\frac{y}{\delta}\right)^{-1} \tag{15}$$

The rate of work dissipation per unit area of the shear band (in the $x0z$ plane) can be found now as

$$\dot{D} = \int_0^\delta (s\dot{\varepsilon}_s + \tau\dot{\varepsilon}_\tau)\,dy \tag{16}$$

where $\dot{\varepsilon}_s = [V]\sin\phi/\delta$, $\dot{\varepsilon}_\tau = [V]/\delta$ and stress state invariants s and τ (Fig. 11(a)) are related to $\dot{\varepsilon}_s$ and $\dot{\varepsilon}_\tau$ through flow rule (11). Finally, the work dissipation rate per unit area of a shear band can be written

$$\dot{D} = M[V] \times\left[\frac{a}{1-n}\left(\frac{\rho_0}{\rho_{max}}\right)^n \frac{(1+A)^{1-n}-1}{A} - b\right] \tag{17}$$

where ρ_0 is the inflow density, $A = \sin\phi\,[V]/V_y^{in}$, and

$$M = 1 - \tan\psi\,\cot\beta_2, \qquad \text{when } 0 \leqslant \psi \leqslant \beta_3$$

$$M = B(1 - \tan\psi\,\cot\beta_1), \qquad \text{when } \beta_3 \leqslant \psi \leqslant \beta_1$$

where

$$B = \frac{\sin\beta_1}{\sin\beta_2}\,\frac{\sin(\beta_2-\beta_3)}{\sin(\beta_1-\beta_3)} \quad \text{and} \quad \tan\psi = \sin\phi$$

Formula (17) was used to obtain the steady state dissipation rate within shear band AB (Fig. 12(a)) and the computational results are rep-

resented by the horizontal sections of the solid diagrams in Fig. 13. Thickness δ of the shear band influences the initial phase of the process, but, once the steady state is reached, the dissipation rate is independent of the band's thickness. Computations were performed for angles α and ψ such that the dissipation rate in steady state was at a minimum. It seems at first that the minimum dissipation rate should be obtained for $\psi = \beta_1(\dot{D} = 0)$. Such solution is inadmissible, however, as it would produce dilation of the material to densities much smaller than the lowest possible density ρ_{min}.

Consider now a mechanism where the discontinuities shown in Fig. 12(a) move down with a certain velocity. Again, the analysis is restricted to shear band AB only. Velocity V_y^{in} now depends on the speed of the shear band's downward translation, the length of the shear band reduces gradually and strains inside the band increase with time. As the shear band moves down from the transition zone, material above the shear band undergoes a continuous deformation process as it enters the converging hopper part of the bunker. X-radiographs suggest that this deformation is incompressible, as no clear dilation effect can be observed above the moving shear bands (see the areas above the top bands in Fig. 6). This deformation will contribute to the total work dissipation. The rate of dissipation within the continuously deforming field was computed approximately, as it was done solely for the purpose of demonstrating the applicability of the proposed analysis (the energy was assumed to be

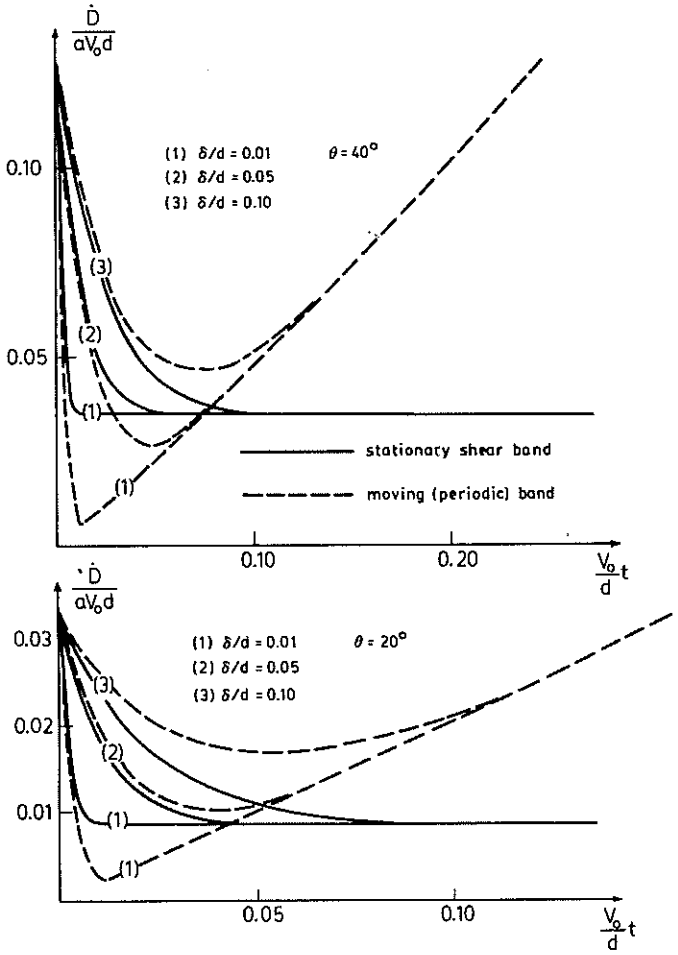

Fig. 13. Work dissipation rate (dimensionless) within shear band A'B' and in area ABB'A' (added together) as function of internal time of process: (a) $\Theta = 40°$; (b) $\Theta = 20°$ ($\beta_1 = 42°$, $\beta_2 = 30°$, $\beta_3 = 20°$, $\rho_0 = 1{\cdot}75$, $\rho_{min} = 1{\cdot}45$, $\rho_{max} = 1{\cdot}90\,Mg/m^3$, $n = 15$)

dissipated within material strip ABB'A' above the band, Fig. 12(a), and the principal stress and strain-rate directions were assumed to be vertical and horizontal). Total rates of work dissipation (within shear band A'B' and area ABB'A') are presented by dashed lines in Fig. 13 as functions of an internal time.

As it was assumed that the shear band underwent rigid translation (no rotation), the distribution of the total strain of the material depends only on the location of a material element across the band (y-co-ordinate). The process was divided into small time increments. The distribution of volume strain of the material inside the shear band was calculated by integrating the volume strain rate (derived from Equation (13)) over the time which a given material element spent inside the shear band. This leads to a piece-wise linear distribution of volume strain across the band. The first range of this distribution (on the 'entrance' side) increases from zero to a certain value. All material elements within this range have entered the shear band during the process of the band's downward propagation. The remaining part of the distribution is constant in space (but variable in time). Material within this constant range has been inside the shear band from the time the shear band was formed. If the process continues for a sufficiently long time, this second (constant) range is reduced to zero, as all the material originally occupying the shear band will have left the band. However, the strain distribution will be constant across the total shear band thickness (though variable with time) if the shear band is of the material type (i.e. $V_y^{in} = 0$).

The distribution of the density was calculated from Equation (12) and parameter k from Equations (9) and (10). The stress parameters τ and s (on the appropriate loading surface, Fig. 11) were calculated, and, the work dissipation rate was computed from Equation (16).

Computations first were performed assuming that band AB is a shock-like band. The lowest gradient of the dissipation rate at the beginning of the process and the lowest dissipation rate during the process were obtained when the propagation speed of the band was equal to that of the material particles above it. The difference between this particular case of a shock-like band and a material shear band is that the latter has an increasing thickness, while the first one is assumed to have a constant δ. Calculations were then repeated assuming that shear band AB is of a material type. The diagrams in Fig. 13 represent dissipation rates for different initial thicknesses of shear band AB (taken as a material shear band). The diagrams show that the thinner the shear band (δ is the initial thickness), the larger the drop in the dissipation rate. If the thickness of the shear band is large as compared to the dimensions of the problem (small size), the steady-state process may yield rates of work dissipation lower than those following from a non-steady, periodic process. This is seen clearly from the diagram for thickness $\delta/d = 0{\cdot}1$ in Fig. 13(a). Whether or not the periodic process yields lower dissipation rates depends also on the geometry of the problem itself. Fig. 13(b) shows the diagrams for the same problem as Fig. 13(a) with only included semi-angle Θ decreased. Now the dissipation rates for both $\delta/d = 0{\cdot}1$ and $\delta/d = 0{\cdot}05$ are higher than those in the steady-state process.

The length of the cycle (dimensionless) is now independent of the band's thickness. This could be predicted without computations. The dissipation rate within the shear band (part of the total dissipation) drops to zero when the density drops to $\rho = \rho_{min}$ (Equations (9) and (10)), and this happens before the end of the cycle. Thus, at the end of the cycle, only the continuously deforming field contributes to the total dissipation, and it is independent of the band's thickness. A yield function that allowed for some hydrostatic pressures at $\rho = \rho_{min}$ would be more realistic.

In both examples presented, the rates of work dissipation at the end of each cyclic perturbation reach levels higher than those in the steady-state analysis. It is the energy dissipation drop at the beginning of the process that determines which mode (steady or non-steady) is going to be activated. Afterwards, if the periodic mechanism is chosen, the process has to follow the admissible pattern of deformation, even if it leads, at some point, to energy dissipation rates exceeding the rates from the steady-state process. A jump from one pattern to the other is kinematically inadmissible.

DISCUSSION OF FINDINGS AND CONCLUSIONS

Strain localization is a common phenomenon in deformation processes of plastic media, yet the fundamental advances in the matter are, so far, applied only to very simple boundary value problems (such as plane strain sample tests). No effective methods exist for solving engineering problems where strain localization could be expected. This Paper demonstrates the possibility of incorporating a strain localization phenomenon into the framework of limit analysis. The question of whether or not the strain localization occurs has not been addressed in this Paper, but a very particular problem pertaining to periodic forming of shear bands was presented. It is essential in this analysis that the mechanisms of deformation are considered as processes where the

shear bands are allowed to propagate, not as incipient flow problems in which the discontinuities are fixed in space.

Based on experimental observations, two kinds of shear band can be distinguished: (*a*) shock-like, and (*b*) material shear bands. Shock-like shear bands are characteristic in that they move with respect to the material. Material particles (grains) enter the shock-like bands, change their relative configuration while passing through them (strain in continuous materials), and leave the bands. These bands are thought to have a constant thickness. Material shear bands, on the other hand, are stationary with respect to the material (i.e. a new material does not enter the bands and the material inside the bands stays inside during the deformation process). If the material dilates in the course of the deformation process, the thickness of the second type of shear band increases. The thickness (or initial thickness) of the shear band is a characteristic material parameter. Introduction of the shear band thickness as a material property (internal length) implies the scale effect, which, indeed, was detected in the examples.

Methods used in the examples for computations of the work dissipation rate within shear bands require some comments. The technique used in the first example was used earlier by the Author to compute dissipation within shock-like shear layers in a pseudo-steady mechanism of pyramidal indentation of strain-hardening metals (Michalowski, 1986). This technique is based on integrating the dissipation rate across thickness δ of the band. In a shock-like shear band (within a continuous material) the yield point varies across the band, as the strain of the material depends on the location inside the band. Thus, in the limit when $\delta \to 0$, a statically inadmissible discontinuity in the stress vector acting on the shear band may occur.

The constitutive model used in description of the material in the second example is the plastic softening–hardening model with the density as the softening parameter. It has been established experimentally that the thickness of shear bands in granular materials is of about 10 grain diameters. The results of computations of the strain (or density) and stress distribution within such range are rather artificial. The scheme presented, however, captures the effect of softening well. Perhaps a constitutive relation in terms of the stress vector and relative displacement increment (or velocity) of the shear band boundaries, with the total relative displacement as a softening parameter, might be more appropriate. Owing to lack of physical data for real materials, such a model was not used in this Paper.

It seems natural to apply the shear band development scheme presented here in the limit analysis formulation of problems. Discontinuities (shear bands) are common features in mechanisms used in the kinematical approach of limit analysis. Although the theorems do not hold for softening–hardening materials, the results following from application of the kinematical approach are well-matched by experiments (Michalowski, 1986) and, as shown in this Paper, this approach can predict cyclic fluctuations not detectable by other techniques.

The technique used in this Paper would not predict fluctuations in velocity fields of extrusion or hopper flow if the material was perfectly plastic or strain-hardening. Indeed, physical experiments suggest that in such cases no periodic fluctuations should be expected (e.g. Butterfield & Andrawes, 1972).

The intent of the Author was not to solve fully the problem of extrusion or that of granular material flow through containers, but to demonstrate the potential capability of the proposed analysis. The minimum material effort hypothesis (minimum work dissipation rate) may have to be replaced in other cases by the minimum applied effort hypothesis, where the minimum of a limit force (or external work rate), rather than a minimum of work dissipation, is sought. For example, in a problem of rigid wedge penetration into a ponderable granular material one should search for the minimum of the force driving the wedge into the material, not for the minimum of internal dissipation.

The method presented in this Paper for analysing the movement of the shear bands in velocity fields is approximate. It is meant as an engineering tool for predicting fluctuations or periodic perturbations in flow mechanisms and is not expected to explain the phenomenon itself.

ACKNOWLEDGEMENTS

The Author would like to express his gratitude to the Underground Space Center, University of Minnesota, for supporting his research, and also to thank Professor A. Drescher, whose X-radiographs are reproduced in this Paper.

REFERENCES

Butterfield, R. & Andrawes, K. Z. (1972). An investigation of a plane strain continuous penetration problem. *Géotechnique* **22**, 597–617.

Drescher, A. & Kang, Y. (1987). Kinematic approach to limit load for steady penetration in rigid-plastic soils. *Géotechnique* **37**, 233–246.

Dresher, A. & Michalowski, R. L. (1984). Density variation in pseudo-steady plastic flow of granular media. *Géotechnique* **34**, 1–10.

Hill, R. & Hutchinson, J. W. (1975). Bifurcation phenomena in the plane tension test. *J. Mech. Phys. Solids* **23,** 239–264.

Michalowski, R. L. (1984). Flow of granular material through a plane hopper. *Powder Technol.* **39,** 29–40.

Michalowski, R. L. (1986). An approximate solution to a problem of pseudo-steady flow of strain-hardening material. *Int. J. Mech. Sci.* **28,** 195–200.

Michalowski, R. L. (1987a). Flow of granular media through a plane parallel/converging bunker. *Chem Engng Sci.* **42,** 2587–2596.

Michalowski, R. L. (1987b). An analytical modeling of kinematical discontinuities in hardening/softening materials. *6th Specialty Conf., Am. Soc. Civ. Engrs Engineering Mechanics Division, Buffalo, NY,* 173.

Michalowski, R. L. (1989). Periodic patterns of granular flow through a plane container. *Proc. 3rd Int. Symp. on Numerical Models in Geomechanics, Niagara Falls,* eds S. Pietruszczak & G. N. Pande, 305–310.

Rudnicki, J. W. & Rice, J. R. (1975). Conditions for the localization of deformation in pressure-sensitive dilatant materials. *J. Mech. Phys. Solids* **23,** 371–394.

Tüzün, U., Houlsby, G. T., Nedderman, R. M. & Savage, S. B. (1982). The flow of granular materials—II. Velocity distributions in slow flow. *Chem. Engng Sci.* **37,** 1692–1709.

Vardoulakis, I. (1980). Shear band inclination and shear modulus of sand in biaxial tests. *Int. J. Numer. Analyt. Meth. Geomech.* **4,** 103–119.

Vermeer, P. A. (1982). A simple shear-band analysis using compliances. *Proc. IUTAM Conference on Deformation and Failure of Granular Materials, Delft,* eds P. A. Vermeer & H. J. Luger, 493–499.